

Subproject A4.6

Metallic Nanostructures by Nanocontact Printing and Templating: Antennas and Receivers

Principle Investigator: Thomas Schimmel

CFN-Financed Scientist: Dr. S. Zhong (3/4 BAT IIa, 18 month)

Further Scientists: Dr. Stefan Walheim, Dr. Matthias Barczewski, Dr. Roland Gröger, Paul Vincze, Tobias Heiler, and Markus Moosmann

**Karlsruhe Institute of Technology (KIT), Campus South
Institute of Applied Physics and
Karlsruhe Institute of Technology (KIT), Campus North
Institute of Nanotechnology**

Metallic Nanostructures by Nanocontact Printing and Templating: Antennas and Receivers

Introduction and Summary

The development of novel photonic and plasmonic devices and technologies such as ultrafast modulators on the basis of silicon, have roused considerable interest recently. In this field, the current world record for the fastest modulator is held by the group of J. Leuthold (A4.4). While the focus of subproject A4.4 (J. Leuthold.) is on devices, their characterization and performance, this subproject A4.6 (Th. Schimmel.) focuses on the development of the required nanolithographic tools, as well as novel materials and thin films with unusual optical properties.

In both areas significant progress was achieved, especially using bottom-up approaches for soft lithography, metal nanowire self-assembly and SCMOL-based materials. The results include:

- **Metallic nanowires made of copper, lead and silver were produced with a variety of structural properties.** With a novel approach, based on self-organization, highly regular periodic arrays of mesoscale wires were fabricated – wire arrays to be used as antennas and outcoupling gratings for thin film optoelectronic devices. Furthermore, freestanding wires with an anomalous high density of twins were synthesized; a new concept leading to a more than 10-fold higher mechanical strength, compared to normal copper bulk material. [A4.6:16, and A4.6:27]
- **Chemosensitive optical gratings were fabricated on the basis of scanning probe lithography.** Dip-Pen Nanolithography was used to produce optical gratings with bio-sensing capability. This novel approach uses the shape change of the liquid crystalline grating upon binding to the analyte, which can be detected in situ by optical means. [A4.6:24]
- **Nano-Contact Printing and Polymer Templating** was used to develop high resolution parallel structuring techniques for metal nanostructures, as required for many A-Projects. High resolution printing yielded a resolution in the 20-nm range, which is suitable for the production of antenna structures [A 4.6:31]
- **High Aspect Ratio Constructive Nanolithography:** polymer brush nanostructures were formed by locally induced constructive Nanolithography with a photo-dimerizable molecule with the tip of an AFM [A 4.6:22]
- **Substrate-Consuming Metal-Organic Layers (SCMOLS) [A4.6:36 and 33] enable the build-up of three-dimensional lithographic structures with cutting edge properties:**
 1. anisotropic material characteristics and
 2. remarkable nonlinear optical properties

This makes SCMOLs ideal candidates for optically active layers in SOI waveguides for ultrafast modulation within subproject A4.4. In collaboration with the group of J. Leuthold, the linear and nonlinear optical properties of various SCMOLS were determined and first devices are being built [A4.6:1], [A4.6:28].

Within this subproject four collaborative diploma theses were completed in 2009 and 2010: Regina Weingärtner and Christopher Wittenberg in collaboration with U. Lemmer, and Matthias Jäger and Robert Palmer with J. Leuthold.

In the timeframe 2006-2010 subproject A4.6 (including the preceding project B1.1) has led to 29 publications and 9 patent applications, among which is 1 article in *Nature Nanotechnology*, 1 in *SMALL*, 1 in *Advanced Materials* and 6 in *Langmuir*.

1. Development of New Specific Methods within this Subproject

1.1 Molecular Editing: Writing with Molecules

The development of bottom-up lithographic methods for the fabrication of three-dimensional organic nanostructures has attracted considerable attention within the last decade. Two possible lithography routes are frequently reported: Step by step mechanically-induced nanografting of only a few monolayers (heights about 5 nm) by subsequent surface reactions [1,2] and surface-initiated polymerization (SIP) (e.g. [3]), which can lead to structure heights above 10 nm. Polymer brush structures are especially attractive because of their multifunctionality. They are known to be stimulus responsive and can effectively suppress/control protein or cell adhesion, for example. Both techniques use multi-step processes, however structures with widths below 100 nm and simultaneously heights above 7 nm could only be achieved by SIP with e-beam patterning of initiator molecule layers (40 nm with an initiator pre-structure width of 10 nm). The spreading of the polymer on the substrate also leads to a rapid line-widening during the growth process.

Our approach is an AFM-based technique to pattern ultrathin organic films, in order to locally initiate chemical follow-up reactions. Our approach of “reversible constructive nanolithography” is based on the site-selective depassivation of parts of a Self-Assembled Monolayer (SAM) by AFM-tip induced molecular exchange. Combining this with a photochemically induced growth process, this monolayer-based lithography directly leads to three-dimensional polymer-brush-like structures, requiring only a single process step. Depending on the exposure time, heights up to 25 nm could be obtained. Only one molecular species is needed for the build-up process, in contrast to other lithographic approaches leading to three-dimensional organic nanostructures. Lithographically defined patterns with line widths down to 40 nm at structure heights of 12 nm were achieved, starting from a primary structure in the first monolayer of 30 nm. This only modest widening means a significant improvement, as compared to earlier SIP-based approaches.

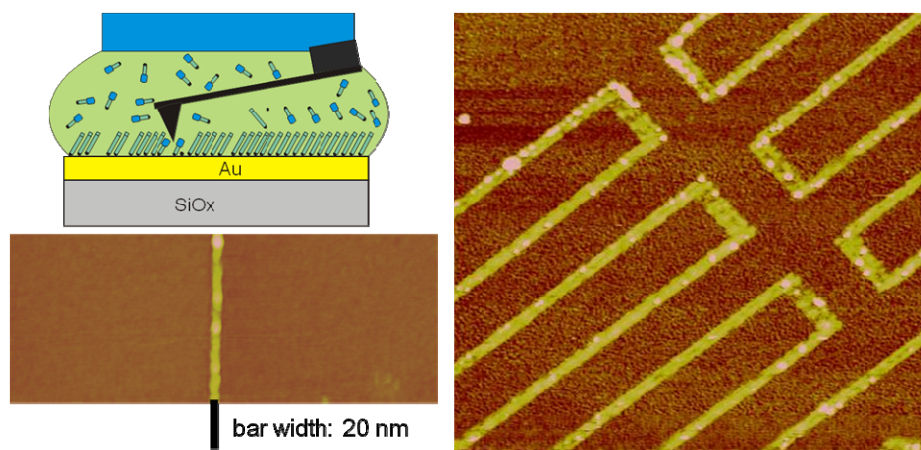


Fig.1 a) After structuring samples in a light-exposed Coumarin-thiol solution ($\lambda > 350$ nm) the AFM-written lines are protruding from the background, in spite of the fact that the inserted molecules are significantly shorter (1.7 nm) than the molecules forming the surrounding ODT SAM (2.4 nm). The cross-section represented in b) reveals, that lines with a height of about 2.5 nm are observed (contact mode AFM in liquid cell) instead of trenches with a depth of 0.8 nm. The typical line width (FWHM) is approx. 20 nm. Allowing longer light-exposure of the solution, lines with heights of 12 nm can be observed (tapping mode, dry sample) having a line width of 40 nm (FWHM). Taken from [A4.6:22].

We utilize a constructive lithographic process, induced locally by the tip of an AFM. Following the tip-induced exchange of molecules, a site-selective constructive reaction leads to the local formation of protruding polymer-brush-like structures. The complete writing and formation is accomplished as a single-step process and the constructive chemistry is shown to be reversible. The lateral resolution of the structures starts at 20 nm (height: 2.5 nm) and scales with the yielded structure height: 12 nm high lines with a width of 40 nm or 23 nm high lines with a width of 85 nm. This scaling is remarkable as compared to that of earlier lithographic approaches with SIP. Lateral stacking of the CDT dimers could hold the polymer chains together leading to an anisotropic growth and therefore to the observed higher aspect ratio. The structures can be selectively deleted by cleaving the disulfide bonds by exposing them to dithioerythritol (DTE), which could be useful for novel molecular lift-off-based processes. Together with the achieved high lateral resolution, our approach of photo-activated constructive nanolithography opens perspectives for the reversible writing of combined topographic and (bio-)functional patterns on the nanometer scale.

1.2 Nano-Contact Printing and Polymer Templating

The novel technique of Nano-Contact Printing (nCP), which we developed recently within the CFN (patent pending), allows the direct printing of a molecular ink with a lateral resolution in the 10 nm range. It is a *parallel* process for the generation of functional nano-patterns. Using a polymer templating technique, recently demonstrated in our group, polymers self-organize by template-guided phase-separation on these patterns. Thus polymer patterns develop by self-organization on the nCP-patterned substrates which, in turn, can be used as resist structures for subsequent dry etching or wet etching processes. Nanostructuring of both metals (including gold films with a thickness of approx. 20 nm) and semiconductors has been recently demonstrated by our group.

Within this subproject a combination of nanoscale structuring (for functional units) and microstructuring (for leads and contact structures) is required, and a parallel fabrication is highly desirable. Therefore, our techniques of Nano-Contact Printing and Polymer Templating, which allow the fabrication of hierarchical micro- and nanostructures using a parallel fabrication process, are ideally suited, especially as they allow the fabrication not only of metallic, but also of semiconducting (e.g. Si) and electrically insulating (e.g. polymers or SCMOL) structures.

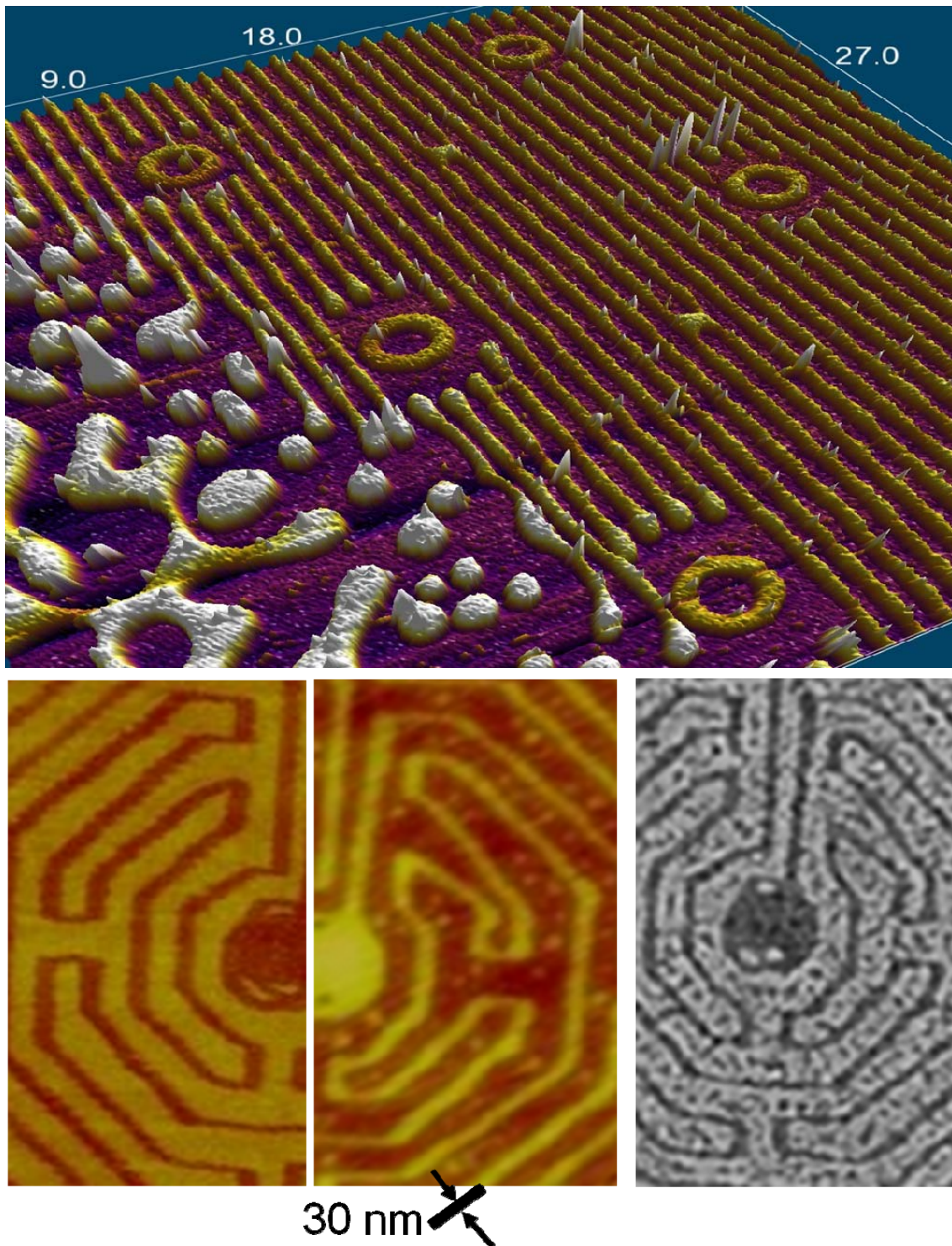


Fig.2: Polymer Blend Lithography (top) and Nano-Contact Printing (nCP) (bottom). The novel, topographically flat nCP stamps enable printing with a resolution in the 20 nm range. The AFM images (bottom left) show the template structure written by molecular editing and the templated block copolymer phase morphology on the underside of the stamp (bottom middle). Etching a gold film, printed by this stamp (nCP), leads to metal nanostructures with the originally designed layout (SEM image bottom right). The printing process could be repeated more than 20 times without loss of resolution. [A4.6:31 and A4.6:21].

The result of the Nano-Contact Printing process can be visualized in the SEM after wet-chemical etching of the printed samples, originally carrying a 20-30 nm thick gold film. The areas protected by the printed SAM are unaffected by the etching, whereby 30 nm wide trenches were etched in areas where the stamps morphology exposed the non-printing polymer phase. The resolution of this novel printing technique is one order of magnitude better than published state of the art micro-contact printing techniques. Nano-Contact Printing solves four of four problems of micro-contact printing:

1. the size limitation due to rupture of delicate structures when the stamp is taken out of the mold;
2. the spreading of ink between adjacent contact regions of conventional stamps;
3. the mechanical problem of bending structures, and
4. the mechanical problem of sagging.

All problems are solved due to the fact that we use a topographically flat stamp which features a lateral phase contrast definition in its ink application capability, instead of contact area definition.

Within project A 4 several collaborations were established using this nanostructuring technique. One of it is the definition of metallic nano-antennas for Project A 4.2 (with U. Lemmer). Here also a collaborative diploma thesis was realized.

2. Components for Devices

2. 1. Self-Organized Metallic Nanowires - a Novel Approach to Plasmonic Devices

Copper nanowires with a high density of traverse twins (twin spacing less than one nm) have been synthesized. These wires spontaneously grow from a pure electrolyte of CuSO_4 by electrodeposition without templates. Such highly twinned metallic nanowires have not been described in literature thus far.

In the field of microelectronics and micro-electro-mechanical systems (MEMS), not only size reduction is needed, but also high electrical conductivity combined with high mechanical strength is required. In order to fulfill these requirements, the introduction of a high density of nanoscale twins into metal nanowires seems to be one of best ways, because twin boundaries as obstacles to dislocations' propagation can dramatically improve mechanical strength, while maintaining a high electrical conductivity at same time. This point has been proven by Lu et al. in copper foils [4]. It is intriguing to know how to introduce and control nanoscale twinning in metal nanowires. Our results are an important step in this direction.

Plasmonic properties of electrochemically grown, as well as SCMOL modified metallic nanowire arrays and individual wires will be investigated, with respect to material, shape and diameter of the various wires (see nano-antenna applications).



Fig.3: Highly twinned Cu-nanowires were synthesized by electrochemical deposition. Their unique microstructure, which was investigated by high resolution TEM, leads to an enormous mechanical strength, proven in situ with advanced FIB techniques. An AFM cantilever (upper right image) was used as force sensor for this measurement. Together with their high electric conductivity, measured by 4-point measurements, this makes them ideal components for plasmonic nano-optical devices. Taken from [A4.6:16].

2.2. Substrate-Consuming Metal-Organic Layers (SCMOLs)

A novel self-organizing class of metal-organic films was discovered in our group [A4.6:33]. Double thiol-functionalized organic molecules produce a metal-organic layer, when brought into contact with coinage metal surfaces like Cu or Ag. The metal is consumed during the growth and the thickness of the final layer depends directly on the thickness of originally evaporated metal film. Three-dimensional metal-organic layers could be produced by self-organization with a model system, consisting of a coumarin-derivative, synthesized at the INT, and pre-structured silver or copper covered substrates. The remarkable layer thickness, in combination with a high lateral accuracy with respect to the template structure, is of a new quality. Because of the substrate-induced growth of the layers, while incorporating the metal atoms of the substrate film, we named them "Substrate-Consuming Metal-Organic Layers" (SCMOL). Various experimental methods were applied to gather information about the growth behavior and the morphology of the model system. A model was established, to consistently explain the observed properties, which is backed by theoretical calculations. Preliminary results indicate that the capability to produce such layers is not limited to the mentioned model system, but extends to a whole class of molecules.

The material properties of the SCMOLs allow for a completely new approach to the production of three-dimensional, z-anisotropic structures from two-dimensional, pre-structured substrates. We developed two types of this "bottom-up lithography". The metal substrates, with thicknesses in the low nanometer range, are structured by covering with laterally defined, 1-2 nm thick monolayers. They are then transformed by an anisotropic growth process into three-dimensional structures with possible thicknesses in the range many hundreds of nanometers. With suitable pre-structuring of the substrate, it is possible to create z-anisotropic features by self-organization, like tunnels within the layers. First experiments with nanoscale pre-structured substrates by "molecular editing" show the ability of this system to produce nanoscale self-organized structures.

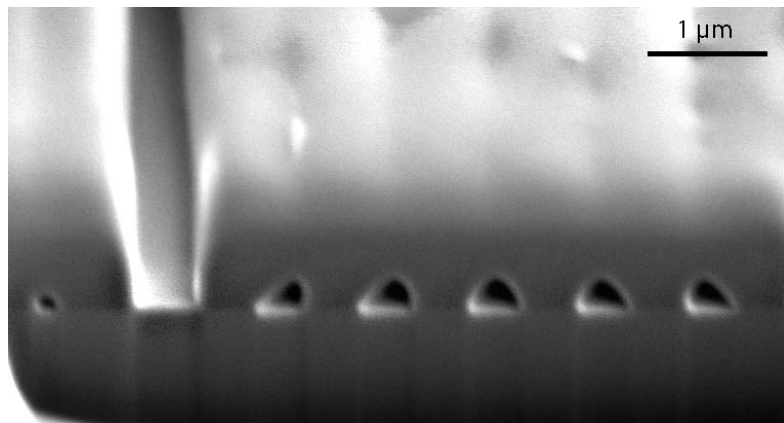


Fig.4: An example of SCMOL lithography: A quasi 2-dimensional metal structure – in this case a 30 nm thick Cu Layer with 15 nm deep trenches – was transformed into a 3-dimensional metal-organic nanostructure. The formation of buried tunnels is unique and a result of the substrate consuming growth mechanism of this novel constructive nanolithography. Taken from [A4.6:33].

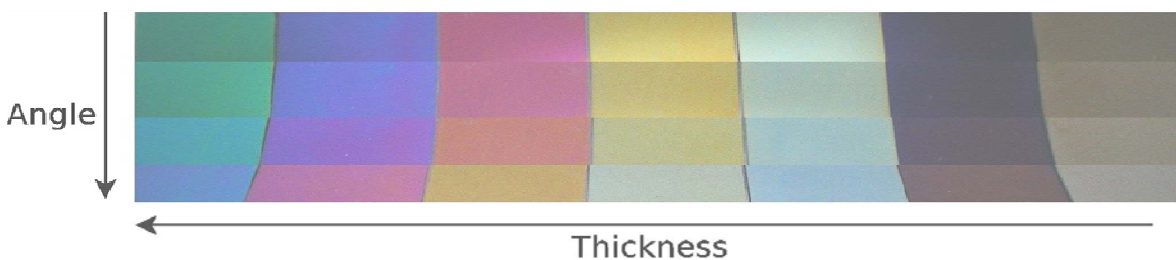


Fig.5: The colors of different SCMOLs on silicon substrates, photographed under different angles. The film thickness was predetermined by evaporating Cu layers with increasing thickness (from left to right) [A4.6:33]

3. Photonic and Plasmonic Devices

3.1 Silicon Waveguides: AFM Investigations

The silicon-on-insulator (SOI) system is expected a promising option for low-cost highly integrated photonic circuits. However, the required technology for fabrication, namely electron beam or deep UV-lithography, as well as inductively coupled plasma etching, is expensive and therefore the privilege of only few laboratories. Furthermore, strongly guiding nanowire waveguides are particularly sensitive to sidewall roughness [5,6], resulting in high propagation losses in the order of

1–2 dB/cm. Recently, it has been shown, that losses can be low when shallow etched ridge waveguides with sub-micrometer waveguide widths or etchless waveguides are used. However, strong mode confinement is the key to high third-order nonlinear effects and is highest when fully etched strip or slot waveguides are used. In close collaboration with the group of Prof. Leuthold (Subproject A4.4) we recently demonstrated and proved that smooth nanowire waveguides can be fabricated by standard contact UV-lithography and preferential etching in aqueous potassium hydroxide solution (KOH). To the best of our knowledge, this is the first report on nanomachining of nanophotonic silicon waveguide structures based on preferential wet etching.

Measurements of trapezoidal waveguides were performed in our group by Atomic Force Microscopy in Tapping Mode. In order to obtain the roughness of the sidewalls, without hitting the sample with the cantilever, samples with multiple waveguides were cleaved parallel to them and tilted by an angle of about 40 degrees. Fig. 6c shows the resulting AFM image of a sidewall of a single waveguide near the brim of the sample. The plane structure on the left side is the sidewall, with a length of about 275 nm. The plane on the right-hand side represents the SiO₂ substrate. The measured RMS values of the side wall roughness varied between 1 nm and 3 nm, depending on the scanned area.

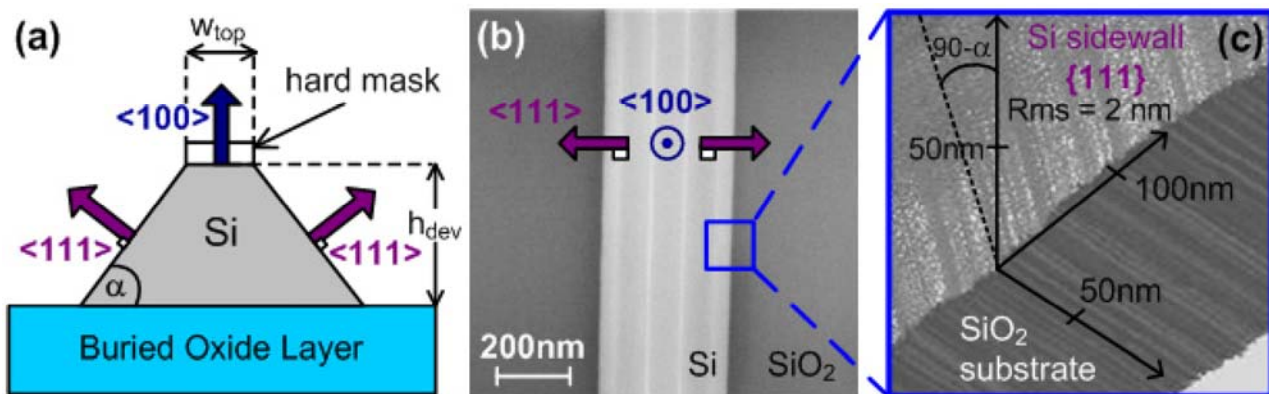


Fig.6 Quantitative AFM characterization of silicon-on-insulator (SOI) nanowire waveguides: Schematic representation (left), SEM (middle) and an AFM image (500 × 500 nm / Tapping Mode, right) of a sidewall of a trapezoidal waveguide. The sample was tilted in order to scan the sidewall horizontally. The measured roughness was between 1.5 nm and 2.5 nm RMS. Taken from [CLEO, Baltimore (USA); Palmer, Leuthold, Moosmann, Schimmel (Submitted Dec. 2010)]

3.2 Surface Plasmon Polariton Absorption Modulator (SPPAM): A first proof of concept

Optical modulators in future integrated circuits should work at 100 GB/s and at best up to 1 TB/s and beyond. Their footprint should be comparable to electronic devices, i.e. they should be in the order and below 1 μm² and compatibility with standard CMOS technology should be guaranteed in order for them to become practical.

Electro-absorption modulators (EAM) belong to the most compact commercially available data encoding devices in optical communications. They are available in typical lengths of 200 μm and with operating speeds up to 40 Gb/s. Unfortunately, junction capacities and carrier related effects fundamentally limit their bandwidth to approximately 60 GHz [7]. Here the feasibility of an electrically controlled compact surface plasmon polariton absorption modulator (SPPAM) has been

demonstrated, operating at 1.55 μm telecommunication wavelength. The device performance is RC-limited with a typical RC-time constant of $\tau = 35$ fs. Therefore, the modulator operation speed theoretically has the potential of exceeding 100 Gb/s and thus fulfilling the future high speed data rate requirements. An extinction ratio of ER=1 dB has been predicted for the modulator with a length of 2 μm and with total plasmonic loss in the range of 18 dB. However, it has been shown that both the extinction ratio and device length can be significantly improved by using Si_3N_4 as an insulator filling the plasmonic gap. An extinction ratio of 1 dB is estimated for the latter case with a 12 dB loss in the device length of less than 0.5 μm , which is obviously comparable to the electronic devices. The structure used for a proof of principle was realized in a close collaboration between the groups of J. Leuthold (A.4.4) and Th. Schimmel (A 4.6).

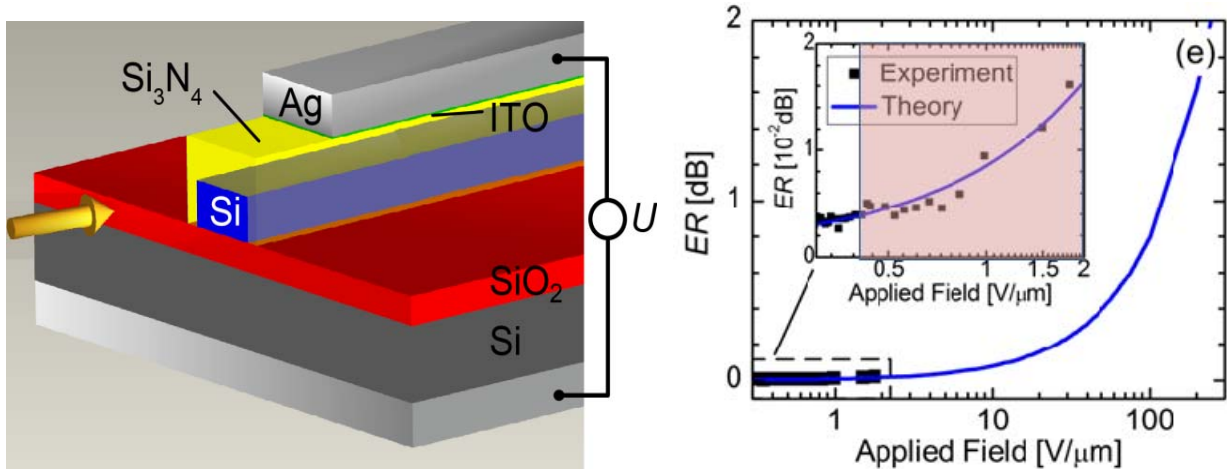


Fig. 7. The configuration of the DUT multilayer structure (left) and the measured extinction ratios over the applied field of the driving electrical signal (right). The extinction ratio calculated by the theory is represented in blue line: fit parameters: $\omega_p = 0.8 \omega_{p0}$ and $\gamma = 2.3 \gamma_0$, where ω_{p0} and γ_0 are the plasma and collision frequencies of ITO. Measuring the values in the highlighted area was possible only after laterally confined etching of the backside of the device, performed at the INT (unpublished).

3.3 SCMOL Nonlinear Optics

The growth process of the SCMOLs has been adopted for the use with SOI chips and the losses of waveguides covered with SCMOL have been reduced. This was done in close collaboration between Prof. Leuthold (M. Jäger, D. Korn, C. Koos) and Prof. Schimmel (P. Vincze, S. Walheim). One of the examined materials, the coumarin derivative CD-SCMOL had very low losses in the visual wavelength range and might be interesting for use at those wavelengths. In the interesting spectral range it has a refractive index of $n \sim 1.65$ and could be used as a waveguide for visual light, if grown on a material with a lower refractive index.

Another of the examined materials is promising for applications at the communication wavelength of 1550 nm. It could be applied to a chip without increasing the loss to a point, where four-wave mixing experiments become impossible.

Preliminary four-wave mixing measurements allow to conclude that the investigated SCMOL have a high third order nonlinearity. The second order nonlinear refractive index makes it interesting as

third order nonlinear material as its n_2 is similar to the one of DDMEBT, a material currently in use as third order nonlinear material.

Finally a reversible effect that allows for the reduction of the material losses of SCMOL by heating the sample has been discovered. This heating can either be applied externally or caused by the absorption of light inside the sample. Strong loss reductions (e.g. from 9.7 dB/mm to 4.4 dB/mm for one of the measured waveguides) have been achieved using this effect. The most probable cause for the loss is water accumulated from the surrounding air.

One of the next steps should be the repetition of the transmission measurements under a controlled atmosphere to prove or disprove water as a cause of the loss. If water is the cause of the loss, heating the sample under protective atmosphere and coating it with a waterproof protection layer, transparent at 1550 nm would lead to a sample with a loss at the lower level. Measurements of four-wave mixing in structures, in which a higher percentage of the light propagates inside the SCMOL layer are planned. These are rib waveguides, operated in TM mode, as well as slot waveguides operated in TE mode.

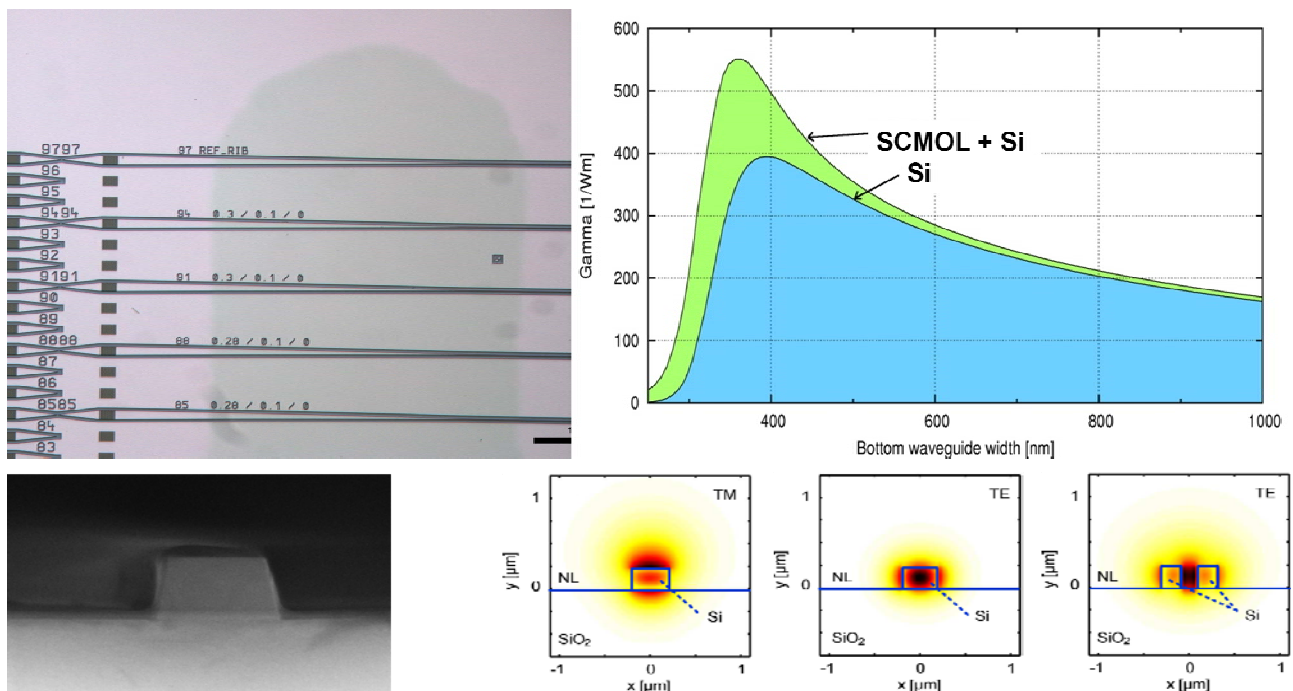


Fig.8: SOI chip, partially covered by a greenish SCMOL layer (top left). Decomposition of the waveguide nonlinearity into the contributions of silicon and SCMOL for different waveguide width (top right). The contributions of silicon and SCMOL are marked in blue and green. The waveguide imaged in the SEM picture has a width of 300 nm (lower left). Mode profiles of TE and TM modes in a SOI rib waveguide are shown in the small images on the bottom right. The image on the right side shows a mode profile of a SOI slot waveguide. The color scale goes from black for high intensities to white for low intensities.

3.4 Novel Optical Sensing Devices

The interaction of electromagnetic waves with matter can be controlled by structuring the matter on the scale of the wavelength of light. Various photonic components have been made by structuring materials using top-down or bottom-up approaches. Dip-pen nanolithography is a scanning-probe-based fabrication technique that can be used to deposit materials on surfaces with high resolution and, when carried out in parallel, with high throughput [8]. In collaboration with the group of S. Lenhart / H. Fuchs (Subproject E 3.2) we show that lyotropic optical diffraction gratings composed of biofunctional lipid multilayers with controllable heights between approx. 5 and 100 nm can be fabricated by lipid dip-pen nanolithography. Multiple materials can be simultaneously written into arbitrary patterns on pre-structured surfaces, to generate complex structures and devices, allowing nanostructures to be interfaced by combinations of top-down and bottom-up fabrication methods. We also show that fluid and biocompatible lipid multilayer gratings allow label-free and specific detection of lipid–protein interactions in solution. This biosensing capability takes advantage of the adhesion properties of the phospholipid superstructures and the changes in size and shape of the grating elements that take place in response to analyte binding.

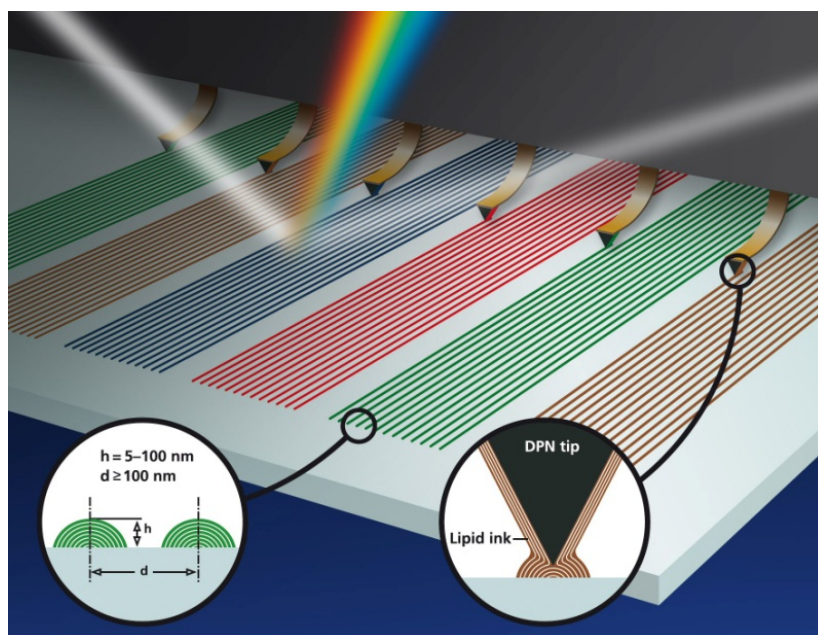


Fig.9: Schematic illustration of the technique used to fabricate lipid multilayer gratings. Parallel AFM tip arrays were used to simultaneously deposit multiple lipids with controllable multilayer thicknesses, laterally structured to form arbitrary patterns (e.g. diffraction gratings) with feature sizes on the same scale as UV, visible or infrared light. In situ observation of the light diffracted from the patterns can be carried out during DPN and used for high throughput optical quality control without the need for fluorescence labels. Taken from [A4.6:24], [A4.6:32].

In conclusion, we have developed a process for the fabrication of photonic structures composed of phospholipid multilayers. It allows direct writing of arbitrary patterns, composed of multiple biocompatible membrane-based materials, on a variety of surfaces, including pre-patterned substrates. The technique is useful for high-throughput biophysical analysis with lipid-based photonic structures and novel photonic sensing elements capable of label-free biosensing by means of a dynamic shape change upon analyte binding. Higher gratings that respond to analyte binding by

a surface-tension change are found to be suitable for detection of analytes at low concentrations, whereas mechanisms based on intercalation of materials into the fluid gratings can expand the dynamic range of sensing, as well as provide a new way to probe dynamic biomembrane function. The bottom-up fabrication method and unique biophysical properties of nanostructured lipid multilayers permits the integration of complex and dynamic biophotonic circuits.

4. Collaborations with other CFN Projects

Subproject A4.6 contributes to several other projects within the CFN, which is also documented by a number of collaborative publications and patents:

- Collobaration with J. Leuthold, Ch. Koos, W. Freude (A4.4): Development and fabrication of waveguide coatings and nanostructures electrodes for high frequency optical modulation [A4.6:1], [A4.6:28]
- Collaboration with H. Fuchs / S. Lenhart (E3.2): Opical gratings - nanolithography [A4.6:24], [A4.6:32].
- Collaboration with U. Lemmer (A4.2): Development of fast, low-cost, parallel fabrication of micron- and submicron electrode structures.
- Collaboration with H. Gliemann / Ch. Wöll (E2.2) [A4.6:26], [A4.6:30].
- Collaboration with S. Linden, M. Wegener (A1.5) on the parallel fabrication of metallic nanoscale structures for photonic metamaterials and plasmonics.
- Providing contact structures for single-atom transistors (Th. Schimmel, B1.6)
- D. Schaadt (sub-project A2.6), for the nanostructuring of semiconductor surfaces and the induced nucleated semiconductor growth on the nanometer scale [A4.6:29].

References

- [1] S. T .Liu, R. Maoz, G. Schmid, J. Sagiv, *Nano Letters* **2** (10), 1055-1060 (2002)
- [2] Liu, J. F.; Cruchon-Dupeyrat, S.; Garno, J. C.; Frommer, J.; Liu, G. Y, *Nano Letters* **2** (9), 937-940 (2002)
- [3] M. Kaholek, W. K. Lee, B. LaMattina, K.C. Caster, S. Zauscher, *Nano Letters* **4** (2), 373-376 (2004)
- [4] L. Lu, Y. Shen, X. Chen, L. Qian, K. Lu, *Science* **304**, 422–422 (2004)
- [5] Y. Vlasov and S. McNab. *Opt. Express* **12**, 1622–1631 (2004)
- [6] C. Poulton, et al. “Radiation modes and roughness loss in high index-contrast waveguides”. *IEEE J. o. Sel. Top., Quantum Electronics* **12**,1306–1321 (2006)
- [7] H. Fukano, T. Yamanaka, M. Tamura, and Y. Kondo, *Journal of Lightwave Technology* **24**, 2219 – 2224 (2006)
- [8] R. D. Piner, J. Zhu, F. Xu, S. H. Hong & C. A. Mirkin, *Science* **283**, 661–663 (1999)